Journal of Sound and Vibration 329 (2010) 3888–3897

Contents lists available at ScienceDirect

Journal of Sound and Vibration

journal homepage: www.elsevier.com/locate/jsvi

Broad band controller design for remote vibration using a geometric approach

Jiqiang Wang [a], Steve Daley [b,*]

[a] College of Energy & Power Engineering, Nanjing University of Aeronautics & Astronautics, 29 Yudao Street, Nanjing 210016, P.R. CHINA
[b] Department of Automatic Control and Systems Engineering, The University of Sheffield, Mappin Street, Sheffield S1 3JD, UK

ARTICLE INFO

Article history:
Received 26 January 2009
Received in revised form
6 February 2010
Accepted 26 March 2010
Handling Editor: D.J. Wagg

ABSTRACT

Over the past three decades, a wide variety of active control methods have been proposed for controlling problematic vibration. The vast majority of approaches make the implicit assumption that sensors or actuators can be located in the region where vibration attenuation is required. However this is either not feasible or prohibitively expensive for many large scale structures or where the system environment is harsh. As a result, optimal control of local vibration may lead to enhancement at remote locations. Controlling remote vibration using only local sensing and actuation is an important concept to resolve this remote vibration control problem. Recently, a geometric methodology that provides an approach for defining the design freedom available for reducing vibrations at both local and remote locations has been proposed by the authors. In an earlier paper, the fundamental results were used to develop design procedures for discrete frequency control; in the current paper, however, the focus is on design procedures for broad band control. A systematic approach is developed that provides an additional design constraint to the geometric methodology to ensure that the resulting compensator provides closed loop stability. The design procedure is illustrated through its application to an active vibration isolation structure.

1. Introduction

Active vibration controller design has reached a high level of maturity following three decades of intensive development and a number of design methods are now well established ([1–6], for example). The majority of approaches assume implicitly that sensing and actuation can be applied in the region where vibration attenuation is ultimately required, however, for many applications this is not feasible. Although it may be possible to recover the lost sensor information with an observer, for example, direct forces often cannot be applied. Such problems are particularly evident in large scale interconnected structures where either the environmental conditions do not allow a wide distribution of sensors and actuators or it is prohibitively expensive to do so. Design based solely on information local to the actuators can result in increased levels of vibration at remote locations. Therefore, the implementation of a locally sub-optimal solution is necessitated for the attainment of a globally optimal one.

On the other hand, controlling remote vibration using only local sensing and actuation is also desirable in many situations since actuators are expensive and/or heavy and are hence avoided in a system design [7]. Hence the study of controlling remote vibration based only on local feedback action is of both theoretical interest and practical significance.

* Corresponding author.
E-mail address: steve.daley@sheffield.ac.uk (S. Daley).

0022-460X/$ - see front matter © 2010 Elsevier Ltd. All rights reserved.
doi:10.1016/j.jsv.2010.03.033

The feasibility of controlling remote vibration using only local sensing and actuation has previously been studied by the authors [8]. A geometric design methodology for discrete frequency (or harmonic) control has been proposed, where the design freedom available for providing both local and remote vibration attenuation is parameterised. In this paper, design procedures for broad band control are presented. Specifically, the problem of disturbance attenuation over an arbitrary frequency band is considered. It is found that an optimal broad band geometric controller can be designed via a linear matrix inequality (LMI) approach. Remarkably, further design freedom can be defined, allowing designers to tune the performance of the optimal geometric controller. The broad band results presented here are important extensions to those obtained in [8] for harmonic control. They result in a systematic design procedure for tackling remote vibration control problem and as a consequence, an optimal controller can be synthesized over an arbitrary frequency band. The presentation in this paper is as follows: the procedures for geometric controller design are presented in Section 2; additional design freedom for tuning the geometric controller is considered in Section 3; the problem of out-of-band performance deterioration is analyzed in Section 4; in Section 5 the proposed design methodology is illustrated through the application to an active vibration isolation system and Section 6 concludes the paper.

2. Geometric controller design

2.1. Preliminaries

It is assumed that the vibrating system can be described by the following frequency response function (FRF):

$$\begin{bmatrix} y(j\omega) \\ z(j\omega) \end{bmatrix} = \begin{bmatrix} g_{11}(j\omega) & g_{12}(j\omega) \\ g_{21}(j\omega) & g_{22}(j\omega) \end{bmatrix} \begin{bmatrix} u(j\omega) \\ d(j\omega) \end{bmatrix} \tag{1}$$

where $y(j\omega)$, $z(j\omega)$, $u(j\omega)$ and $d(j\omega)$ represent the locally measured vibration, the remote vibration, the control force and the disturbance force, respectively. The control aim is to achieve reductions in both $y(j\omega)$ and $z(j\omega)$ (where possible) over an arbitrary frequency band $[\omega_1,\omega_N]$ through application of the feedback control law:

$$u(j\omega) = -k(j\omega)y(j\omega) \tag{2}$$

In the case that a measurement of $z(j\omega)$ is not available during implementation, it is assumed that the transfer function matrix:

$$G = \begin{bmatrix} g_{11}(j\omega) & g_{12}(j\omega) \\ g_{21}(j\omega) & g_{22}(j\omega) \end{bmatrix} \tag{3}$$

can be obtained during a commissioning phase. It is seen that the system model, Eq. (1), together with controller, Eq. (2), can be represented by the linear fractional transformation description (Fig. 1) that is commonly used in modern H_∞ and H_2 design procedures. But it will be seen that the design procedure developed here can retain important information about solution existence and design freedom.

2.2. Introduction to geometric controller design

Denote the sensitivity and complementary sensitivity at a discrete frequency $\omega=\omega_0$ by$S(j\omega_0)$ and $T(j\omega_0)$, respectively. By defining the following equations:

$$\alpha(j\omega_0) = S(j\omega_0) - 1 = -T(j\omega_0) \tag{4}$$

and

$$\alpha(j\omega_0) = \beta(j\omega_0)g(j\omega_0) \quad \text{with} \quad g(j\omega_0) = \frac{g_{11}(j\omega_0)g_{22}(j\omega_0)}{g_{12}(j\omega_0)g_{21}(j\omega_0)} \tag{5}$$

it can be shown [8] that reduction in $y(j\omega)$ and $z(j\omega)$ for the discrete frequency $\omega=\omega_0$ is equivalent to satisfying the following conditions, respectively:

$$|\alpha(j\omega) + 1| < 1 \tag{6}$$

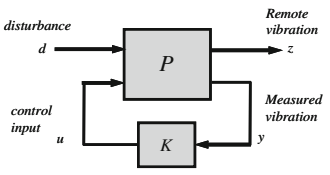

Fig. 1. Linear fractional transformation representation.

and

$$|\beta(j\omega)+1|<1 \tag{7}$$

From the observation that Eq. (5) relating $\alpha(j\omega)$ and $\beta(j\omega)$ defines a Möbius transformation, it is clear that the mapping of Eq. (7) on complex α-plane is a circle (and its interior) with centre at $-g(j\omega_0)$ and radius $|g(j\omega_0)|$. Hence it can be concluded that simultaneous reduction of $y(j\omega)$ and $z(j\omega)$ is achievable for this discrete frequency $\omega=\omega_0$ if and only if the mapping of the unit circle (and its interior) $|\beta(j\omega)+1|<1$ on the complex α-plane intersects the unit αcircle (and its interior) $|\alpha(j\omega)+1|<1$, and the corresponding reduction is scaling with respect to each circle. Finally it is noted that an optimal line joining $(-1,0)$ with $(-g(j\omega_0))$ on the complex α-plane can be defined and desired levels of attenuation can be obtained by choosing an appropriate point on the line, e.g. a choice at point $-g(j\omega_0)$ provides infinite attenuation in $z(j\omega_0)$. These fundamental results have been exploited to develop a design methodology for harmonic control by the authors in [8].

The aim of reducing $y(j\omega)$ and $z(j\omega)$ over an arbitrary frequency band $[\omega_1,\omega_N]$ can be approached on a frequency-by-frequency basis. However, it is noted that the optimal choice α_{opt} is to be varied from one frequency to the next over the desired frequency band $\omega\in[\omega_1,\omega_N]$ and this results in an optimal trajectory on the complex α-plane. These observations are illustrated in Fig. 2.

However it is not true to state that a compensator then exists that can provide simultaneous reduction across an arbitrarily wide range of frequencies, since closed loop stability is not considered. It turns out (Proposition 5 in [8]) that internal stability will be guaranteed if $\alpha_{\text{opt}}(j\omega)$ is a mapping of a stable function, provided that $g_{11}(j\omega)$ is minimum phase. As a result the optimal broad band geometric controller can be obtained from $k(s)=-\alpha(s)/([\alpha(s)+1]g_{11}(s))$, which follows from the definition of sensitivity. Thus the question that needs to be answered is how to find such a stable transfer function $\alpha(s)$ given the optimal choice α_{opt} over any target frequency band $[\omega_1,\omega_N]$. This is considered in the following section.

2.3. Obtaining an optimal broad band geometric controller via LMIs

Given the data points resulting from the optimal choice α_{opt} over $[\omega_1,\omega_N]$, the problem of fitting a stable transfer function $\alpha(s)$ to these points consists of two sub-problems: one is the existence problem, or the possibility of finding a stable transfer function $\alpha(s)$ that interpolates the data points; the other is the optimization problem, namely finding the best approximation to the given data points in the event of a failure to provide exact interpolation. The existence problem turns out to be a Nevanlinna–Pick interpolation problem, which widely occurs in robust identification, signal processing and circuit theories [9,10]. The answer to this is provided by a modified Pick condition as shown in [11]:

Existence problem. : A stable transfer function $\alpha(s)$ that interpolates the optimal choice α_{opt} over $[\omega_1,\omega_N]$ exists if and only if the following Pick matrix P

$$P=\left[\frac{1-\alpha_k\overline{\alpha_l}/M^2}{j(\omega_k-\omega_l)+2a}\right]_{1\le k,l\le N} \tag{8}$$

is positive definite, where α_i is the optimal choice $\alpha(j\omega_i)$ for frequency $\omega_i\ \forall i\in[1,N]$; a and M are positive real numbers defining the minimal degree of stability and maximum modulus of $\alpha(s)$ on the half plane $\Re(s)\ge -a$ (or more accurately $M\ge\sup_{\Re(s)\ge-\alpha}|\alpha(s)|$), respectively.

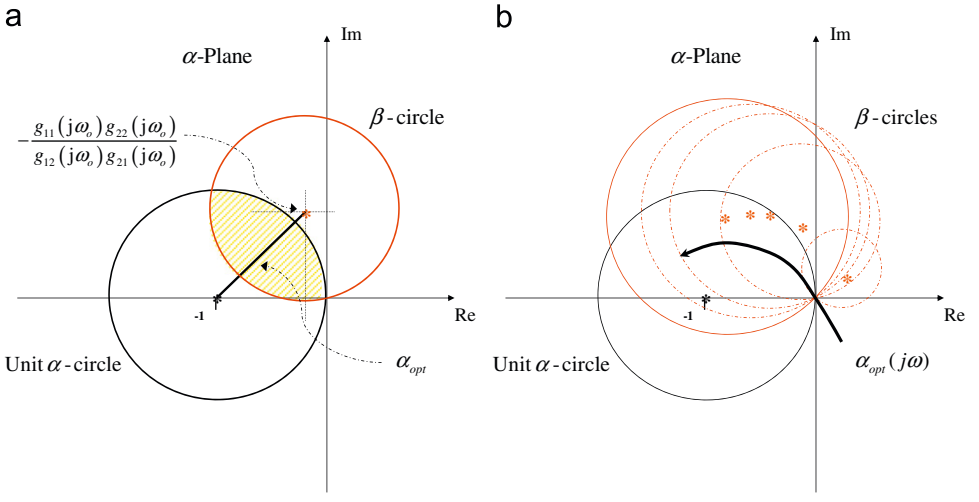

Fig. 2. (a) Mapping of $|\beta(j\omega)+1|<1$ on the complex α-plane for a frequency ω_0 and (b) optimal solution $\alpha_{\text{opt}}(j\omega)$ on the complex α-plane for broad band control.

Optimization problem. : When the Pick matrix above fails to be positive definite, there does not exist a stable transfer function $\alpha(s)$ that interpolates exactly through the optimal choice $\alpha(j\omega_i)$ $\forall i \in [1,N]$. The problem of finding the best approximation to the data points proves to be provided by a series of linear matrix inequalities (LMIs). This is obtained in [11] by defining $T_0 = \left[\frac{1}{j(\omega_k-\omega_l)+2a}\right]_{1\le k,l\le N}$ *and* $Q = \text{blockdiag}(\frac{\alpha_1}{M},\ldots,\frac{\alpha_N}{M})$ and then the Pick Matrix P can be rewritten as

$$P = T_0 - QT_0Q* \tag{9}$$

where * is the Hermitian operator. It follows from the Schur complement lemma that P is positive definite if and only if

$$\begin{bmatrix} T_0 & Q \\ Q* & T_0^{-1} \end{bmatrix} > 0 \tag{10}$$

Eq. (10) together with those LMIs defining the uncertainty around each data points α_i for frequency ω_i, when presented with an LMI solver [12], provides the best approximation to the optimal choice $\alpha(j\omega_i)$ over the frequency band $[\omega_1,\omega_N]$. The desired stable transfer function $\alpha(s)$ can then be obtained from the interpolation data (see [13] for its transfer function or state-space representation). By the definition of sensitivity the broad band geometric controller is thus $k(s) = -\alpha(s)/([\alpha(s)+1]g_{11}(s))$.

Remark. : For optimal choice $\alpha(j\omega_i)$ with complex values, the resulting stable transfer function can have complex coefficients. A method that can be utilized to produce a real, rational and stable transfer function runs as follows: augment the complex conjugate values of $\alpha(j\omega_i)$ into the interpolating set and solve the N-P problem, resulting in complex-valued $K(s)$; then $k(s) = (K(s)+K*(s))/2$ is the desired real, rational and stable transfer function that interpolates the desired optimal choice $\alpha(j\omega_i)$ over $[\omega_1,\omega_N]$, where $K^*(s)$ is $K(s)$ with complex coefficients replaced by their complex conjugates.

3. Performance tuning

For any design methodology it can be very important to provide additional freedom to tackle objectives beyond the main design goal. But it is also important to be able to describe the effects of design freedom in terms of system performance. The optimal choice α_i defines directly the levels of attenuation in $y(j\omega)$ and $z(j\omega)$. It is also noted that the Pick condition introduces additional design parameters, namely the minimal degree of stability a and the maximum modulus M of $\alpha(s)$ on the half plane $\Re(s) \ge -a$. Their introduction arises from the determination of the existence of a stable transfer function $\alpha(s)$ that interpolates exactly through the optimal choice $\alpha(j\omega_i)$ $\forall i \in [1,N]$. The consequence is that a stable $\alpha(s)$ cannot be found to interpolate $\alpha(j\omega_i)$ when the Pick matrix fails to be positive definite. Hence an approximation to the optimal choice $\alpha(j\omega_i)$ has to be made to obtain a stable $\alpha(s)$ (to ensure internal stability). In the following it is shown that a and M can be used to increase the accuracy of the approximation and hence improve performance of the broad band geometric controller $k(s)$ within the targeted frequency band $[\omega_1,\omega_N]$.

Denote the ith eigenvalue of P by λ_i, which is a real number following from the fact that P is Hermitian; then a fundamental theorem from linear algebra states that the sum of eigenvalues is equal to the matrix trace. That is

$$\sum_{i=1}^{N}\lambda_i = \text{trace}(P) = \frac{N - \sum_{k=1}^{N}|\alpha_k|^2/M^2}{2a} \tag{11}$$

Thus $\sum_{i=1}^{N}\lambda_i$ is monotonic with respect to a or M. Hence increasing M or decreasing a can increase the "positiveness" of $\sum_{i=1}^{N}\lambda_i$. With a large enough M or small enough a, the Pick matrix can eventually become positive definite and therefore allows an exact interpolation with a stable $\alpha(s)$ to the optimal choice $\alpha(j\omega_i)$ $\forall i \in [1,N]$. This leads to the following tuning rule:

Tuning rule: The performance of the broad band geometric controller $k(s)$ within the target frequency band $[\omega_1,\omega_N]$ can be refined by decreasing a or increasing M.

However caution is required since on allowing the stability margin a to be small the system becomes more vulnerable to instability and in addition, on allowing the maximum modulus M of $\alpha(s)$ on the half plane $\Re(s) \ge -a$ to be large the performance outside the targeted frequency band $[\omega_1,\omega_N]$ can be "potentially" sacrificed. To see this, it is noted that the maximum deterioration in $y(j\omega)$ and $z(j\omega)$ is determined by the H_∞ norm of $\alpha(j\omega)+1$ and $\beta(j\omega)+1$. But

$$\|\alpha(j\omega)+1\|_\infty \le \|\alpha(j\omega)\|_\infty + 1 < M+1 \tag{12}$$

This is so since from definition $M \ge \sup_{\Re(s)\ge -a}\alpha(s)$ and by the maximum modulus principle we have

$$M \ge \sup_{\Re(s)\ge -a}|\alpha(s)| > \sup_{\Re(s)=0}|\alpha(s)| = \sup|\alpha(jw)| = \|\alpha(jw)\|_\infty \tag{13}$$

The maximum deterioration in $z(j\omega)$ is

$$\|\beta(j\omega)+1\|_\infty = \|\frac{\alpha(j\omega)}{g(j\omega)}+1\|_\infty \le \|\alpha(j\omega)\|_\infty \|\frac{1}{g(j\omega)}\|_\infty + 1 < MN+1 \tag{14}$$

where $\|1/g(j\omega)\|_\infty \equiv N$.

From Eqs. (12) and (14) it is seen that out of band deterioration in $y(j\omega)$ and $z(j\omega)$ for the worst case can be alleviated by decreasing M. However the tuning rule elaborated above states that performance of the broad band geometric controller and hence in-band-performance can be improved by increasing M. It is strongly emphasized that this is not a compromise that has to be made between in-band and out-of-band performances: increasing M can improve the in-band performance but not necessarily deteriorate the out-of-band performance. This is so since improvement of in-band performance refers to the "closeness" with a desired specification while out-of-band deterioration expresses the fact that disturbances cannot be reduced over all frequencies. The latter is often termed as a "waterbed effect" associated with non-minimum-phase plants [14] or more generally Bode's sensitivity integral theorem [15].

By asserting that re-design M has no cause-and-effect relationship with the out-of-band performance deterioration, it is immediately pointed out that out-of-band deterioration as embodied in Bode's integral theorem is a fundamental design limitation that cannot be resolved by any advanced controller design method. An understanding of this limitation will be very helpful for geometric broad band controller design and the phenomenon of out-of-band deterioration. This is examined in the next section and we conclude this section by pointing out that the above tuning rule retains its usefulness as a design guide.

4. Out of band deterioration

The problem of performance deterioration out of the targeted frequency band is closely related to a fundamental limitation imposed by feedback control structure, namely that expressed by Bode's integral theorem. For a system whose loop transfer function is stable with at least 2-pole roll-off, this theorem can be expressed as [16]

$$\int_0^\infty \ln|S(j\omega)|d\omega = 0 \tag{15}$$

where $S(j\omega)$ is the sensitivity function. As pointed out in the last section, this unity requirement puts a fundamental constraint on feedback design that is not conquered by any advanced feedback controller design method. Many control design puzzles can be explained through this unity constraint. In the broad band geometric controller design methodology elaborated above, it is thus pondered that there might exist fundamental limitations on both sensitivity $S(j\omega)$, which is a measure of reduction in local vibration $y(j\omega)$, and the quantity $(\beta(j\omega)+1)$, which is a measure of reduction in remote vibration $z(j\omega)$. Indeed, such limitations exist and can be quantified by the design freedom α. Denote the set of solutions of $\alpha=-1$ in $\mathrm{Re}\, s>0$ by $\{m_i\}$, the set of solutions of $\alpha=-g$ in $\mathrm{Re}\, s>0$ by $\{n_i\}$ and the remote vibration reduction by $R(j\omega)$. Further assume α has at least 2-pole role-off[1]; then the following fundamental results hold.

Theorem 1. *The reduction in local vibration $y(j\omega)$ is constrained by the following integral relationship*:

$$\int_0^\infty \ln|S(j\omega)|d\omega = \pi\sum \mathrm{Re}(m_i) \tag{16}$$

Theorem 2. *If α/g has at least 2-pole role-off, the reduction in remote vibration $z(j\omega)$ is constrained by the following integral relationship*:

$$\int_0^\infty \ln|R(j\omega)|d\omega = \pi\sum \mathrm{Re}(n_i) \tag{17}$$

Proof. Denote $S_{\mathrm{mp}}(s)$ and $S_{\mathrm{ap}}(s)$ as the minimum-phase and all-pass partitions of $S(s)$, respectively; then it can be shown (Lemma 3, p. 96, [14]) that for every point $s_0=\sigma_0+j\omega_0$ with $\sigma_0>0$

$$\ln|S_{\mathrm{mp}}(s_0)| = \frac{1}{\pi}\int_{-\infty}^{\infty} \ln|S(j\omega)|\frac{\sigma_0}{{\sigma_0}^2+(\omega-\omega_0)^2}d\omega \tag{18}$$

Taking $\omega_0=0$ results in

$$\ln|S_{\mathrm{mp}}(\sigma_0)| = \frac{1}{\pi}\int_{-\infty}^{\infty} \ln|S(j\omega)|\frac{\sigma_0}{{\sigma_0}^2+\omega^2}d\omega \tag{19}$$

That is

$$\frac{\pi}{2}\sigma_0\ln|S_{\mathrm{mp}}(\sigma_0)| = \int_0^{\infty} \ln|S(j\omega)|\frac{{\sigma_0}^2}{{\sigma_0}^2+\omega^2}d\omega \tag{20}$$

Taking the limit of the above equation as $\sigma_0\to\infty$, we have

$$\int_0^\infty \ln|S(j\omega)|d\omega = \frac{\pi}{2}\lim_{\sigma_0\to\infty}\sigma_0\ln|S_{\mathrm{mp}}(\sigma_0)| \tag{21}$$

[1] From Eq. (4), the relationship between loop transfer function L and α can be expressed as $\alpha=-L/1+L$. Hence α has the same pole roll-off rate as L.

Noting that $S_{mp}(s)=S(s)/S_{ap}(s)$, Eq. (21) can be rewritten as

$$\int_0^\infty \ln|S(j\omega)|d\omega = \frac{\pi}{2}\lim_{\sigma_0\to\infty}\sigma_0 \ln|S(\sigma_0)| - \frac{\pi}{2}\lim_{\sigma_0\to\infty}\sigma_0 \ln|S_{ap}(\sigma_0)| \tag{22}$$

By definition $S(\sigma_0)=1+\alpha(\sigma_0)$; also since α has at least 2-pole role-off, $\alpha(\sigma_0)\approx A/\sigma_0^k$ for some constant A and $k\geq 2$ as $\sigma_0\to\infty$. Hence from the Maclaurin's series expansion, $\ln(1+\alpha(\sigma_0))=\frac{A}{\sigma_o{}^k}-\frac{A^2}{2\sigma_0{}^{2k}}+\cdots$

Therefore the first term of the right hand side of Eq. (22) converges to zero as$\sigma_0\to\infty$. Eq. (22) now reads

$$\int_0^\infty \ln|S(j\omega)|d\omega = -\frac{\pi}{2}\lim_{\sigma_0\to\infty}\sigma_0 \ln|S_{ap}(\sigma_0)| \tag{23}$$

Since the zeros of the sensitivity function are the set of solutions of $\alpha=-1$, $S_{ap}(\sigma_0)$ in the above equation can therefore be expressed as

$$S_{ap}(\sigma_0)=\prod_i \frac{\sigma_0-m_i}{\sigma_0+\overline{m}_i} \tag{24}$$

Eq. (23) can thus be rewritten as

$$\int_0^\infty \ln|S(j\omega)|d\omega = -\frac{\pi}{4}\lim_{\sigma_0\to\infty}\sigma_0\sum_i\left[\ln(1-\frac{2\mathrm{Re}(m_i)}{\sigma_0}+\frac{|m_i|^2}{\sigma_0^2})-\ln(1+\frac{2\mathrm{Re}(m_i)}{\sigma_0}+\frac{|m_i|^2}{\sigma_0^2})\right] \tag{25}$$

Applying again the Maclaurin's series expansion leads to

$$\int_0^\infty \ln|S(j\omega)|d\omega = -\frac{\pi}{4}\sum_i\lim_{\sigma_0\to\infty}\sigma_0\left[-\frac{2\mathrm{Re}(m_i)}{\sigma_0}-\frac{2\mathrm{Re}(m_i)}{\sigma_0}+\cdots\right] \tag{26}$$

That is

$$\int_0^\infty \ln|S(j\omega)|d\omega = \pi\sum_i \mathrm{Re}(m_i) \tag{27}$$

This proves Theorem 1 □.

On the other hand, from Eq. (7) it is clear that $R(j\omega)=1+\beta(j\omega)$, which is simply a definition of the level of reduction in the remote vibration $z(j\omega)$. With the help of Eq. (5) we have

$$R(j\omega)=1+\frac{\alpha(j\omega)}{g(j\omega)} \tag{28}$$

Therefore the set of unstable zeros of $R(s)$ is $\{n_i\}$, and hence all-pass part of $R(s)$ can be expressed as

$$R_{ap}(s)=\prod_i \frac{s-n_i}{s+\overline{n}_i} \tag{29}$$

Therefore if α/g also has at least 2-pole role-off, the procedures in proving Theorem 1 can be reproduced here to validate Theorem 2.

In Eqs. (16) and (17), both $\mathrm{Re}(m_i)$ and $\mathrm{Re}(n_i)$ are positive; therefore the best situation for reduction in local vibration $y(j\omega)$ and remote vibration $z(j\omega)$ is expressed by

$$\int_0^\infty \ln|S(j\omega)|d\omega = 0 \tag{30}$$

and

$$\int_0^\infty \ln|R(j\omega)|d\omega = 0 \tag{31}$$

Hence both local vibration $y(j\omega)$ and remote vibration $z(j\omega)$ cannot be suppressed over all frequencies and this is the ultimate reason for out-of-band performance deterioration.

5. Example: geometric controller design for an active vibration isolation system

5.1. Active vibration isolation structure

Fig. 3 shows an idealised three-degree-of-freedom active vibration isolation mount. In a typical application, not only would the vibration in m_z caused by the disturbance d be required to be minimized to protect the payload, but also the transmitted vibration in m_y should be optimized to reduce the force transmitted to the receiving structure (denoted by the solid rectangle in Fig. 3). In the following, the geometric broad band controller design methodology is illustrated by its application to this system, assuming that control is applied only at m_y, for example through the use of an inertial actuator.

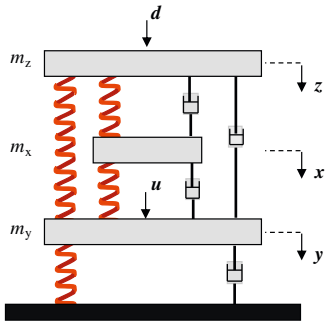

Fig. 3. An active vibration isolation system.

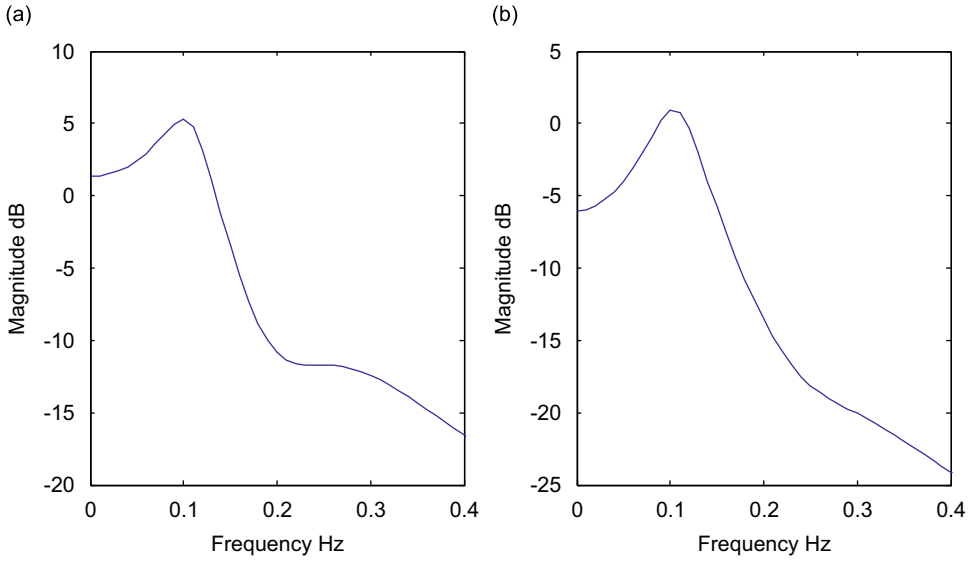

Fig. 4. (a) Remote disturbance response $z(j\omega)$ and (b) disturbance transmission.

The system considered has mass, stiffness and damping matrices as follows:

$$M=\begin{bmatrix}1&0&0\\0&1&0\\0&0&1\end{bmatrix},\ C=\begin{bmatrix}4&-1&-2\\-1&1&0\\-2&0&2\end{bmatrix}\ \text{and}\ K=\begin{bmatrix}4&-1&-1\\-1&2&-1\\-1&-1&2\end{bmatrix}$$

The system can be readily written in the form of (1):

$$\begin{bmatrix}y(j\omega)\\z(j\omega)\end{bmatrix}=\begin{bmatrix}g_{11}(j\omega)&g_{12}(j\omega)\\g_{21}(j\omega)&g_{22}(j\omega)\end{bmatrix}\begin{bmatrix}u(j\omega)\\d(j\omega)\end{bmatrix}$$

5.2. Design broad band geometric controller

Fig. 4(a) shows the frequency response of remote vibration z to excitation by disturbance d (the plot is therefore of $|g_{22}(j\omega)|$). It can be seen that the first resonance occurs at 0.1 Hz and this leads to a peak in the transmission path, as can be seen in the m_y response to the same forcing ($|g_{12}(j\omega)|$) in Fig. 4(b).

Therefore a control scenario can be considered where the objective is to provide optimum reduction in m_z (z: remote location) without increasing vibration in m_y (y: local end) over a frequency band, e.g. $[0.06, 0.14]$ Hz centred on the resonance at 0.1 Hz. The optimal choice (the data points over $[0.06, 0.14]$ Hz) can be computed from elementary geometric arguments by considering the relative locations of the α-circle and β-circle illustrated in Fig. 2. With the assumption $a=0.25$ and $M=3$, it is found that the Pick matrix is not positive definite and therefore the Pick condition is violated, and hence the initial optimal choice is infeasible. The application of the above optimization over LMIs, while setting the real and imaginary parts of uncertainty for the initial data set to be uniformly bounded within 0.08, results in a "new" feasible

optimal choice. With this new feasible optimal choice, the closed-loop as well as the open-loop FRFs are illustrated in Fig. 5. Also shown are the closed-loop FRFs that would have resulted from the original optimal choice, had this been feasible. The deviation between the two closed-loop FRFs reveals the accuracy of the approximation and hence the loss relative to the theoretical performance. It is clear that the deviation in achieving the feasible solution is very small. The design procedure proposed is therefore practically viable.

5.3. Tuning geometric controller performance

Now increase the value $M=3$ to 4 while still assuming $a=0.25$ with uncertainty bound 0.08 in the above example, it is found that the Pick condition is still violated, and hence the initial optimal choice is still infeasible. The application of the above optimization over LMIs results in another new set of feasible optimal points. The resulting closed-loop FRFs are compared as illustrated in Fig. 6. It can be seen that the accuracy of approximation has increased and so the loss relative to the theoretical performance becomes smaller. Finally it is noted that when M increases to $M=6$ or a decreases to $a=0.15$, the Pick matrix becomes positive definite and this which results in an exact interpolation and hence no loss relative to the theoretical performance. The tuning rule thereby indeed retains its usefulness as a design guide. This validates the results presented in Section 3.

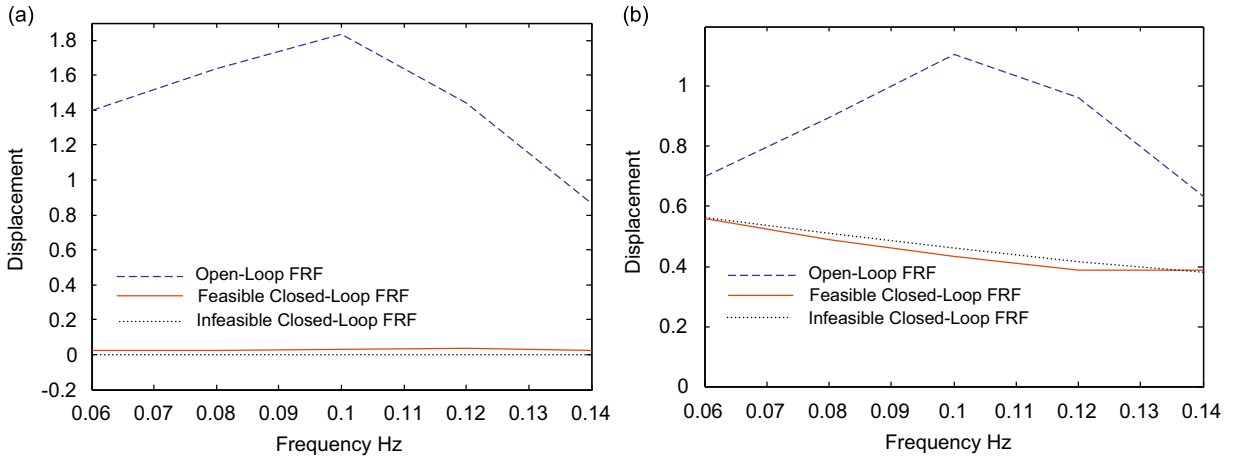

Fig. 5. Open-loop and closed-loop FRFs with feasible and infeasible optimal choice: (a) remote vibration z and (b) local vibration y.

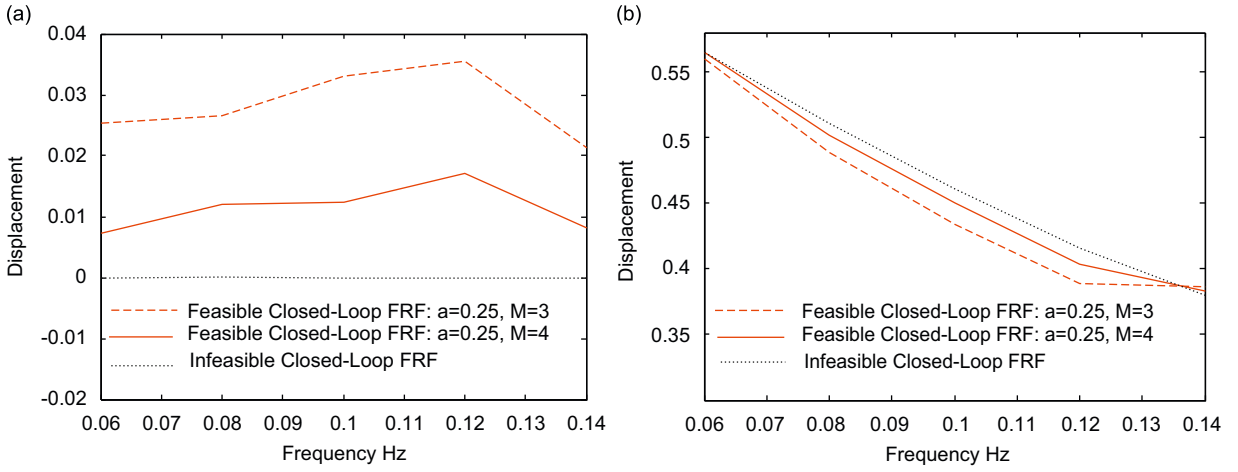

Fig. 6. Tuning of geometric broad band controllers for (a) remote vibration z and (b) local vibration y—comparison of closed-loop FRFs with different a and M pairs. Dotted line is the original infeasible optimal choice and hence can be seen as a reference when a and M pair is tuned. It is seen that increasing M can improve accuracy of approximation and hence broad band controller performance in relation to the prescribed specification.

5.4. Out of band deterioration and controller simulation

Since the resulting interpolating transfer function has a 2-pole roll-off and the unstable solution of $\alpha = -1$ is 41.42 then from Theorem 1

$$\int_0^\infty \ln|S(j\omega)|d\omega = 41.42\pi \tag{32}$$

Meanwhile α/g has a 4-pole roll-off and there are 4 unstable solutions of $\alpha = -g$ at $0.01 \pm 0.9448j$ and $0.014 \pm 0.352j$ then from Theorem 2:

$$\int_0^\infty \ln|R(j\omega)|d\omega = 0.048\pi \tag{33}$$

The particular numbers in the right hand side of the above equations are not the main concern since the area can be balanced over an infinitely wide frequency range. But they do reflect some design preferences, e.g. a large number can well indicate there is either performance deterioration over a wide frequency band or a large peak over a certain narrow frequency band. Fig. 7 shows the open and closed loop performance over the whole frequency band. It can be seen clearly that performance deterioration exists both for the local vibration y and the remote vibration z.

Finally, Fig. 8 shows simulation results for the geometric broad band controller. The broad band disturbance is simulated as a random disturbance passing through a band-pass filter. With reference to the theoretical performance shown in Fig. 5, it can be seen that the method has successfully enabled an extension of the geometric design approach for control of remotely located vibrating systems to the broad band case.

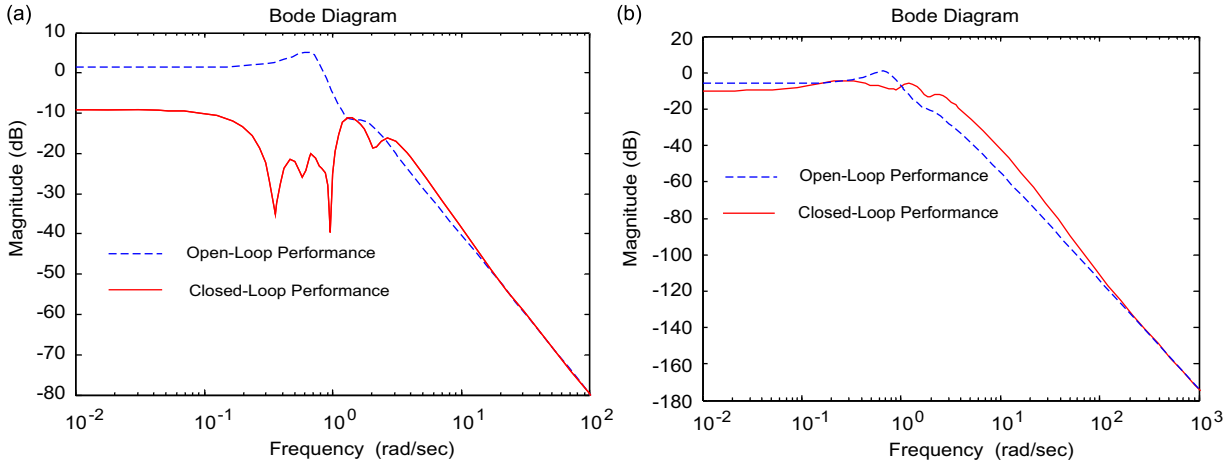

Fig. 7. Whole-band geometric controller performance: (a) remote vibration z and (b) local vibration y.

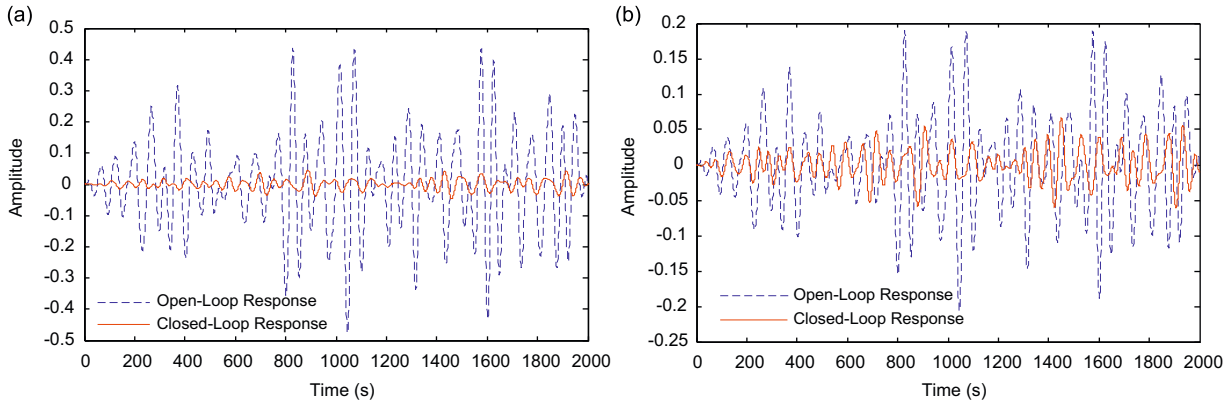

Fig. 8. Geometric controller performance: (a) remote vibration z and (b) local vibration y.

6. Conclusions

A geometric methodology has been developed for broad band control of remotely located vibrating systems. This method is particularly targeted at situations where it is required to apply control at a particular point on a structure but sensors and actuators are located only at some remote location. The approach results in a straightforward design strategy where design freedom can be directly related to system performance. A calculation of feasible controllers is carried out via convex optimization over LMIs. These theoretical considerations have been validated through their application to the broad band control of vibration in an active vibration isolation system.

References

[1] P.A. Nelson, S.J. Elliott, *Active Control of Sound*, Academic Press, London, 1992.
[2] C.R. Fuller, S.J. Elliott, P.A. Nelson, *Active Control of Vibration*, Academic Press, London, 1996.
[3] J. Shaw, N. Albion, Active control of the helicopter rotor for vibration reduction, *Journal of the American Helicopter Society* 26 (1981).
[4] L.A. Sievers, A.H. von Flotow, Comparison and extensions of control methods for narrow band disturbance rejection, *American Society of Mechanical Engineers NCA* 8 (1990) 11–22.
[5] S.J. Elliott, I.M. Stothers, P.A. Nelson, A multiple error LMS algorithm and its application to the active control of sound and vibration, *IEEE Transactions on Acoustics, Speech and Signal Processing* 35 (1987) 1423–1434.
[6] S. Daley, J. Hätönen, D.H. Owens, Active vibration isolation in a 'smart spring' mount using a repetitive control approach, *IFAC Journal of Control Engineering Practice* 14 (2006) 991–997.
[7] I. Fantoni, R. Lozano, *Non-linear Control for Underactuated Mechanical Systems*, Springer, 2001.
[8] S. Daley, J. Wang, A geometric approach to the design of remotely located vibration control systems, *Journal of Sound and Vibration* 318 (4-5) (2008) 702–714.
[9] J. Partington, *Interpolation, Identification and Sampling, London Mathematical Society Monographs*, vol. 17, Oxford University Press, 1997.
[10] A. Bultheel, D. De Moor, Rational approximation in linear systems and control, *Journal of Computational and Applied Mathematics* 121 (2000) 355–378.
[11] J. Wang, S. Daley, A geometric design approach to the broad band control of remotely located vibration, in: Proceedings of the 15th Mediterranean Conference on Control and Automation, Greece, 27–29 June, 2007.
[12] MATLAB Robust Control Toolbox: LMI, The Mathworks, Inc.
[13] C. Coelho, L. Silveira, J. Philips, Passive constrained rational approximation algorithm using Nevanlinna–Pick interpolation, in: Proceedings of the Conference on Design, Automation and Test in Europe, 2002, pp. 923–931.
[14] J.C. Doyle, B.A. Francis, A.R. Tannenbaum, Feedback Control Theory, Macmillan, New York, p. 92.
[15] A. Megretski, Multivariable Control Systems, MIT Lectures Notes, 2004.
[16] C. Mohtadi, Bode's integral theorem for discrete-time systems, in: IEE Proceedings, vol. 137, Pt. D, No. 2, March 1990.